Conduction in Bacterial Films

Spectroscopic Slicing to Reveal Internal Redox Gradients in Electricity-Producing Biofilms**

*Luciana Robuschi, J. Pablo Tomba, Germán D. Schrott, P. Sebastián Bonanni, P. Mariela Desimone, and Juan Pablo Busalmen**

Exocellular electron conduction is one of the most fascinating discoveries of microbiology in the last decade. In natural and man-made environments it is thought to play a fundamental role, allowing the exchange of electrons between bacterial cells[1] and between these and external electronic acceptors.[2] Moreover, it is one of the fundamental processes behind the production of electricity by electroactive biofilms grown on electrodes, which are of paramount importance in such emerging technologies as microbial fuel cells,[3] microbial electrolysis cells,[4] the microbial electrosynthesis process,[5] and whole cell biosensors.[6]

Electroactive biofilms grown on polarized electrodes are in fact a very appropriate system for exploring electron conduction because researchers have learnt to grow them in fully controlled conditions with excellent reproducibility.[7] In the typical case, biofilms of *Geobacter sulfurreducens*, the most efficient current producer described to date, are grown on a polarized electrode during 4–6 days until obtaining a constant current. During this time, cells reproduce actively at maximal rate, using the electrode as the electron acceptor, until reaching a thickness of about 40–60 μm. At this stage, cells within the entire population seem to operate at an uniform rate, as evidenced by the constant increase in the accumulation of proteins.[7b] A remarkable feature in these biofilms is that a uniform distribution of cell activity can only be possible if cells at a distance from the electrode are electrically connected to it by a low-resistance pathway that prevents electron acceptor limitations. There is debate as to whether such electron conduction is based on one of two alternative mechanisms: metallic-like conduction through nanowires,[8] or electron hopping (superexchange) through cytochromes.[9] In metallic-like conduction, electrons are proposed to delocalize in a network of pilin A, thanks to

a resonance effect of aromatic groups in the protein structure. Electron hopping, on the other hand, is proposed to occur from heme to heme groups of adjacent cytochrome molecules, provided a critical intermolecular spacing in the order of Ångstroms is present.

Both electron transport pathways have an intrinsic resistance that, depending on its magnitude, may produce a potential decay that will result in a measurable redox gradient across the biofilm. In this regard, it was recently demonstrated that electron transport from cells to the electrode is driven by the presence of a redox gradient within the biofilm.[10] Interestingly, recent modeling results[11] predict the existence of such redox gradient in the context of the superexchange model. Besides, previous evidences from UV/Vis spectroscopy suggest the existence of reduced cytochromes in the upper layers of biofilms,[12] which in principle is only possible in the presence of a relatively high internal biofilm resistance. All of these data are in conflict with high biofilm conductivity values supposed to be conferred by pili filaments,[8] according to which the variation in the fraction of oxidized compounds will be hardly detected with the available technology.[11] In this scenario, measuring the potential gradient across biofilms in vivo becomes extremely relevant, because it can provide information about limitations to current production, while it can also help in the definition of the mechanism that most appropriately describes biofilm conduction.

Linking electrochemical techniques with spectroscopic analysis has been particularly relevant in biofilm research. Surface-enhanced infrared absorption (SEIRA) spectroscopy has been instrumental in the identification of cytochromes as the molecules responsible for wiring cells to the electrode,[13] surface-enhanced Raman (SER) spectroscopy has provided more details about these molecules,[14] and transmission UV/Vis spectroscopy has helped in the analysis of redox changes in biofilms under electrochemical control.[7d,12,15] All of these techniques are based on the absorption (IR, UV/Vis) or scattering (Raman) of energy by molecular bonds and allow the identification of molecules by their characteristic fingerprint spectrum. In the particular case of electricity-producing biofilms, all of the available spectroscopic information points to cytochromes as the molecules responsible for the spectral changes and relates these changes with their electrochemical redox response. Spectroscopic techniques with confocal resolution have the potentiality of spatially resolve distribution or variations of the local redox state of cytochromes, thus informing about internal biofilm physiology.

In a first experimental approach to explore spatial redox electrochemistry inside biofilms, Virdis et al. have shown that

---

[*] L. Robuschi, G. D. Schrott, P. S. Bonanni, Dr. J. P. Busalmen
Laboratorio de Bioelectroquímica, División Corrosión, INTEMA-CONICET
Juan B. Justo 4302, B7608FDQ, Mar del Plata (Argentina)
E-mail: jbusalme@fi.mdp.edu.ar

Dr. J. P. Tomba, P. M. Desimone
Laboratorio de Microespectroscopía, División Polímeros, INTEMA-CONICET
Juan B. Justo 4302, B7608FDQ, Mar del Plata (Argentina)

Supporting information for this article is available on the WWW under http://dx.doi.org/10.1002/anie.201205440.

changes in the vibrational properties of biofilm cytochromes owing to changes in the redox status of the proteins can be detected, non-invasively, with confocal Raman microscopy (CRM).[16] Herein CRM is used to monitor biofilm growth ex situ, and the potential use of the technique for analyzing redox gradients within the biofilm is proposed. In the same line of thinking, and aiming to gain information on structural and physiological features of electricity-producing biofilms, we have constructed an electrochemical cell that can be mounted on the stage of an optical microscope. The cell is designed to use thin film transparent indium tin oxide (ITO) working electrodes, thus allowing the observation of biofilms in situ and in vivo through the electrode (Supporting Information, Figure S1). By using CRM, the redox state of molecules at different planes of biofilms producing current can be explored. Besides, complementary information about the three-dimensional (3D) structure and thickness of the biofilm can be gained in a non-invasive way by optical slicing with a phase contrast microscope.

ITO is the material of choice for spectroelectrochemical research owing to its negligible absorption in the UV/Vis range of light and its conductive properties. As previously shown by others,[7d,12,15] biofilms of *G. sulfurreducens* can grow on ITO electrodes following typical kinetics and reaching a stable current of about 5–6 A m^{-2} after about day 12 (Supporting Information, Figure S2b), closely agreeing with results obtained on graphite electrodes.[7b] Measuring the biofilm thickness in situ during the time of growth reveals that produced current scales linearly with thickness up to about 40 μm, but intriguingly reaches a limiting value after that point in spite of a thickness increment threefold (Supporting Information, Figure S2c). Optical slicing of stabilized populations complements this observation showing that biofilms are markedly irregular along the *Z* axis, exhibiting a region with high density of cells that expands over 20–40 μm from the electrode (Figure 1). Beyond this limit, biofilms become less dense, and produce pillar structures of up to 120–130 μm
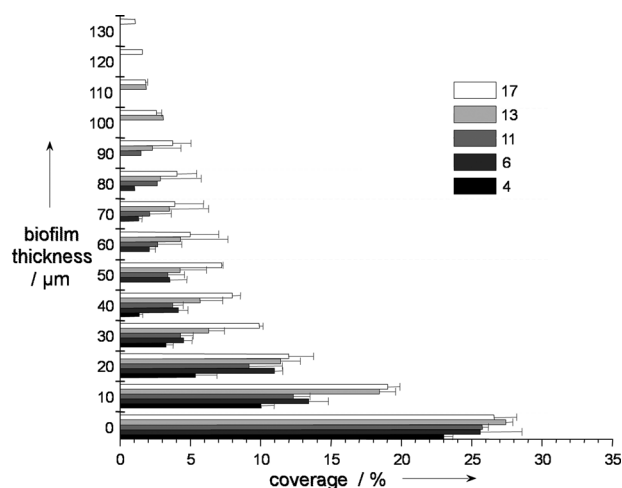

Figure 1. Percentage of area covered by cells in biofilm focal planes at increasing distances from the ITO electrode surface after 4 (black), 6 (dark gray), 11 (gray), 13 (light gray), and 17 days (white) of growth under −0.15 V polarization. Coverage data are the mean value of three different optical fields; bars indicate standard deviation.

towards the solution. On the base of this structural data, it is hypothesized that different physiologies may be operating at regions with different cell density, with most active cells densely packed near the electrode.

Cell activity is considered here as respiratory activity in relation to current production and can be probed at each biofilm layer from the measurement of the redox state of cells using IR or Raman vibrational spectroscopy. In the experiments presented herein, we have selected CRM, exploiting the sensitivity of Raman absorption to conformational changes in redox molecules and the superb spatial resolution of confocal optics for biofilm slicing.

The Raman spectral profile of the fully developed biofilms at the electrode interface level depends on the applied potential (Supporting Information, Figure S3a). At an oxidizing potential (that is, 0.05 V Ag/AgCl, 3 M NaCl), Raman peaks at 1311, 1360, 1400, 1540, and 1585 cm^{-1} dominate the spectrum. Peaks at 1311 and 1540 are characteristics of amide groups as can be found in proteins. Furthermore, peaks at 1360, 1400, and 1585 cm^{-1}, along with some other minors at 1564 and 1638 cm^{-1}, can be ascribed to resonant excitation of heme groups of c-type cytochromes. These bands, which are typically associated with stretching of atomic bonds of the porphyrin ring, have been reported to be very sensitive to changes in the oxidation state of the metal atom.[17] Remarkably, upon total electrochemical reduction at −0.65 V, the whole spectrum intensity increased and bands associated with c-type cytochromes changed in relative intensity.

Although the spectral pattern of reduced biofilms is markedly different to that observed for the oxidized counterpart, changes in features of individual bands are not as dramatic as those reported in studies of pure isolated c-type cytochrome forms.[14] This is reasonable in the context of overlapping contributions from the variety of c-type cytochromes that are known to participate in electron transport through biofilms. To overcome limitations in tracking changes of single Raman bands, we used a method of component analysis that allowed us to account for the information of the whole spectral profile and resolve contributions from reduced and oxidized forms. Overall, any of the spectra obtained at different potentials were effectively reconstructed from a linear superposition of totally oxidized (spectrum at 0.05 V) and totally reduced (spectrum at −0.65 V) forms, plus a polynomial function to account for changes in baseline (Supporting Information, Figure S3b). The analysis yields the contribution of each of those forms, which is directly connected with relative amounts of the two oxidation states. The dependence of the molar fraction of reduced and oxidized cytochromes with potential closely agree with that measured for the evolution of current, giving support to the calculation.

Using the same algorithm, the fraction of reduced species at any location into the biofilm can be calculated from each of the local Raman spectrum. Of main interest for the aims of this work, changes can be profiled along the *Z* dimension under polarization, providing information about the steady state reduction level during current production. Changes in the fraction of reduced species along the *Z* axis are presented

in Figure 2 for polarization potentials located above, below, and at the midpoint potential of the biofilm redox signal (−0.40 V; Supporting Information, Figure S3c). Under −0.65 V polarization, cells cannot use the electrode as the
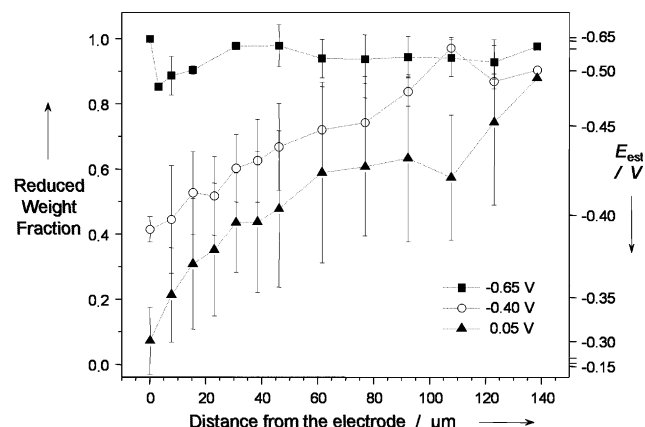

Figure 2. Evolution of the fraction of reduced species with the distance to the electrode in a biofilm polarized at −0.65 (■), −0.40 (○), and 0.05 V (▲) vs. Ag/AgCl, 3 M NaCl, as calculated from Raman spectra by component analysis (see text). E_{est}: potential values estimated from data in the Supporting Information, Figure S3c. Bars indicate standard deviation between two independent biofilms.

electron acceptor, and electrons accumulate in outer membrane cytochromes.[7c] The fraction of reduced cytochromes is maximal in this situation, regardless the distance to the electrode surface. At −0.40 V the fraction of reduced cytochromes decreases to about 40% at the surface level, as expected for an applied potential in the range of the midpoint potential of the biofilm redox signal. Interestingly, the fraction of reduced cytochromes increases with increasing distance from the surface, reaching values of up to 0.9 at 60 μm. Upon increasing the potential to 0.05 V the entire redox profile of biofilms moves towards the oxidized side. Notably, although at this potential cytochromes at the interface are virtually fully oxidized, reduced cytochromes are still observed in upper layers of the biofilm (that is, beyond about 30–40 μm), even when a large overpotential is applied (Supporting Information, Figure S3c). From a physiological point of view, cells near the electrode are expected to be very active at 0.05 V being able to respire at maximal rate. This is in accordance with structural data in Figure 1, showing that cell density is higher below about 30 μm from the surface, where, according to Figure 2, 50% of cytochromes are able to accept respiratory electrons (that is, oxidized). On the other hand, owing to the lack of oxidized cytochromes, respiration by cells in upper layers is expected to be limited to a maintenance (basal) rate (Figure 2).[11] As basal respiration cannot support cell growth, the result is a limitation in the development of cell clusters that leads to an open biofilm structure (Figure 1). It is interesting to note that a lack of electron acceptor in the upper layers of the biofilm have been recently predicted by numerical modeling by considering electron hopping as the mechanism of electron conduction,[11] which together with the information presented herein

strongly indicates that electron conduction proceeds at least in some extent, by electron hopping.

Finally, of main importance for current research in the field, by limiting biofilm thickness and lowering the respiration rate of cells far from the electrode, the redox gradient diminishes the current density produced by the biofilm. In this scenario, finding a strategy to reduce this potential loss along the Z axis would help to produce thicker and more active biofilms that may lead to achieve economically sustainable bioelectrochemical systems.[18]

Experimental Section

Biofilms of *G. sulfurreducens* were anaerobically grown on electrodes in continuous culture at an applied potential of −0.15 V using a custom-made thin-film electrochemical cell (Supporting Information, Figure S1). Sodium acetate was added as the carbon source and electron donor to a modified fresh-water media described elsewhere.[7c]

Biofilm thickness and coverage were measured using a Nikon Eclipse T*i*-U inverted microscope with a motorized Z axis and a 60× objective with a distance correction ring (ULWD Nikon) in phase contrast mode (See the Supporting Information).

Chronoamperometry was performed using an Autolab PGSTAT 101 potentiostat controlled by the NOVA 1.6 dedicated software. Tin-doped indium oxide (ITO) coated glasses were used as the working electrode. The counter electrode was a platinum wire and the reference was a BASi RG6 Ag/AgCl, 3 M NaCl electrode (0.209 V vs. SHE). The exposed working electrode area was 0.32 cm^2.

Confocal Raman spectra were recorded with a Renishaw in Via Reflex spectrometer system equipped with charge-coupled device (CCD) detector of 1040 × 256 pixels and coupled to a Leica microscope with a computer-controlled *x-y-z* stage, using the same objective used for optical microscopy. An Ar laser line (514 nm, 50 mW) was used as excitation source in combination with a grating of 2400 grooves/mm. Laser power was kept below 10% to avoid biofilm damage. Depth profiling was carried out by focusing the laser spot (Ø: 15 μm) at successively deeper position within the biofilm, starting from the ITO-biofilm interface. Data reproducibility is shown in the Supporting Information, Figure S3d. The Z scale reported in Figure 2 has been corrected from refraction aberrations by including a rescaling factor of 1.5.[19]

[1] Z. M. Summers, H. E. Fogarty, C. Leang, A. E. Franks, N. S. Malvankar, D. R. Lovley, *Science* **2010**, *330*, 1413.

[2] D. R. Lovley, T. Ueki, T. Zhang, N. S. Malvankar, P. M. Shrestha, K. A. Flanagan, M. Aklujkar, J. E. Butler, L. Giloteaux, A.-E. Rotaru, D. E. Holmes, A. E. Franks, R. Orellana, C. Risso, K. P. Nevin in *Advances in Microbial Physiology*, Vol. 59 (Ed.: K. P. Robert), Academic Press, New York, **2011**, pp. 1.

[3] B. E. Logan, *Nat. Rev. Microbiol.* **2009**, *7*, 375.

[4] H. Liu, S. Grot, B. E. Logan, *Environ. Sci. Technol.* **2005**, *39*, 4317.

[5] K. Rabaey, R. A. Rozendal, *Nat. Rev. Microbiol.* **2010**, *8*, 706.

[6] U. Schröder, *J. Solid State Electrochem.* **2011**, *15*, 1481.

[7] a) K. Fricke, F. Harnisch, U. Schröder, *Energy Environ. Sci.* **2008**, *1*, 144; b) E. Marsili, J. Sun, D. R. Bond, *Electroanalysis* **2010**, *22*, 865; c) G. D. Schrott, P. S. Bonanni, L. Robuschi, A.

Esteve-Nuñez, J. P. Busalmen, _Electrochim. Acta_ **2011**, _56_, 10791;
d) Y. Liu, H. Kim, R. R. Franklin, D. R. Bond, _ChemPhysChem_
2011, _12_, 2235.

[8] N. S. Malvankar, M. Vargas, K. P. Nevin, A. E. Franks, C. Leang,
B.-C. Kim, K. Inoue, T. Mester, S. F. Covalla, J. P. Johnson, V. M.
Rotello, M. T. Tuominen, D. R. Lovley, _Nat. Nanotechnol._ **2011**,
_6_, 573.

[9] a) S. M. Strycharz-Glaven, R. M. Snider, A. Guiseppi-Elie, L. M.
Tender, _Energy Environ. Sci._ **2011**, _4_, 4366; b) D. R. Bond, S. M.
Strycharz-Glaven, L. M. Tender, C. I. Torres, _ChemSusChem_
2012, _5_, 1099.

[10] R. M. Snider, S. M. Strycharz-Glaven, S. D. Tsoi, J. S. Erickson,
L. M. Tender, _Proc. Natl. Acad. Sci. USA_ **2012**, _109_, 15467.

[11] P. S. Bonanni, D. F. Bradley, G. D. Schrott, J. P. Busalmen,
ChemSusChem **2012**, DOI: 10.1002/cssc.201200671.

[12] Y. Liu, D. R. Bond, _ChemSusChem_ **2012**, _5_, 1047.

[13] J. P. Busalmen, A. Esteve-Núñez, A. Berná, J. M. Feliu, _Angew._
Chem. **2008**, _120_, 4952; _Angew. Chem. Int. Ed._ **2008**, _47_, 4874.

[14] D. Millo, F. Harnisch, S. A. Patil, H. K. Ly, U. Schröder, P.
Hildebrandt, _Angew. Chem._ **2011**, _123_, 2673; _Angew. Chem. Int._
_Ed._ **2011**, _50_, 2625.

[15] A. Jain, G. Gazzola, A. Panzera, M. Zanoni, E. Marsili,
Electrochim. Acta **2011**, _56_, 10776.

[16] B. Virdis, F. Harnisch, D. J. Batstone, K. Rabaey, B. C. Donose,
Energy Environ. Sci. **2012**, _5_, 7017.

[17] T. G. Spiro, T. C. Strekas, _J. Am. Chem. Soc._ **1974**, _96_, 338.

[18] T. H. J. A. Sleutels, A. Ter Heijne, C. J. N. Buisman, H. V. M.
Hamelers, _ChemSusChem_ **2012**, _5_, 1012.

[19] J. P. Tomba, M. de La Paz Miguel, C. J. Perez, _J. Raman Spec-_
trosc. **2011**, _42_, 1330.